ICMIEE-PI-140405

Experimental and Numerical Analysis of Fluid Flow through an Orifice Meter

Md. Tanbin Hasan Mondal [1,*] , *Md. Mostafizar Rahman* [2] , *Dr. Mihir Ranjan Halder* [3]
[1, 2, 3] Department of Mechanical Engineering, Khulna University of Engineering & Technology, Khulna-9203, BANGLADESH

ABSTRACT
An orifice meter is a differential pressure flow meter which reduces the flow area using an orifice plate. Orifice meter is a device commonly used for measuring fluid flow in industrial purposes such as metering flow in the natural gas industry. Experimental and numerical computations of pressure drop (ΔP) and coefficient of discharge (C_d) in an orifice are presented in this paper. Marker and Cell (MAC) algorithm is used for numerical computation. Standard κ-ε model is used for turbulent quantities. The numerical computations are done for the range of Reynolds number $3.3X10^4$ to $4.6X10^4$. Numerical computation is calibrated computing the fully developed length and it is found to have the fully developed length as (138x0.05) or 6.9. Numerically the coefficients of discharge are found 0.61, 0.63 and 0.64 respectively. The coefficients of discharge are also found from experimentation for the same dimensions and input parameters of numerical computation as 0.62, 0.64 and 0.65 respectively for the corresponding flows of numerical solution. In this study the experimentally obtained values of coefficient of discharge are always found higher by 1.95%, 1.56% and 1.54% respectively than that of numerical computation.

Keywords: Orifice meter, MAC algorithm, κ-ε model, Numerical model, Coefficient of discharge.

1. Introduction

An orifice meter is a differential pressure flow meter which reduces the flow area using an orifice plate [1]. The orifice plate is inserted between two flanges perpendicularly to the flow, so that the flow passes through the hole with the sharp edge of the orifice pointing to the upstream. Orifice meter is commonly used for measuring fluid flow in industrial purposes such as metering flow in the natural gas industry. The popularity of the orifice meter can be attributed primarily to its simplicity, relatively low cost and little maintenance requirements in comparison to other fluid meters. In this paper, the study of water flow through an orifice meter by both numerically and experimentally has been presented. This type of fluid flow problem can be solved by computational fluid dynamics (CFD) [2]. For this problem MAC algorithm is chosen to use. The MAC algorithm method is one of the earliest and most useful methods for solving full Navier-stokes equations [4]. It was basically developed to solve problems with free surface flows but can be applied to any incompressible fluid flow problem. The numerical computations are done for the range of Reynolds number $3.3X10^4$ to $4.6X10^4$. An experimental set up has been fabricated with a pipe diameter, 0.05 m, pipe length, 4.5 m, and an orifice diameter, 0.025 m and tested in the laboratory. The pressure drops in the orifice meter and the corresponding coefficients of discharge for flow through the orifice meter have been determined.

2. Model Details

The theoretical analysis refers to a typical orifice meter as shown in Fig.1. The entry of liquid to the orifice meter is in axial direction [5]. Conservation equations for axisymmetric flow of water through the orifice meter were solved simultaneously satisfying the respective boundary conditions by an explicit finite difference computing technique developed by Hirt and Cook following the original MAC (Marker and Cell) method due to Harlow and Welch. The steady state solution of top flow was achieved by advancing the equations in time till the temporal derivatives of all the variables fall below a pre-assigned small quantity ∂ [3]. The standard k-ε model has been adopted for the computation of turbulent flow. The space derivatives of the diffusion terms were discretized by the central differencing scheme while the advection terms were discretized by the hybrid differencing scheme based on the local peclet number Pe associated with the cell. A 66X36 variable sized adaptive grid system was considered with clustered cells near the inlet and orifice. The variations in the size of grids were made uniformly. It was checked by further refinement of the cells (with doubling and quadrupling the number of grids in both the directions) but did not show the change in velocity (both axial and tangential) components and turbulent kinetic energy by more than 2% [4].

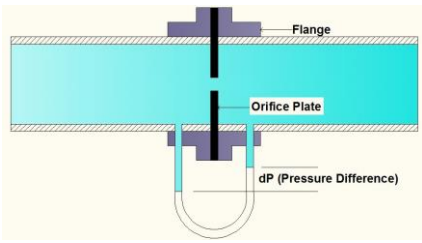

Fig.1 Schematic diagram of a short square-edged orifice inserted in a smooth run pipe

2.1 Governing Equations

The governing equation for this flow situation is simplified considering axisymmetric flow in cylindrical polar coordinate system (r, θ, z). Assuming unit angle in θ direction, the governing equations in dimensionless

* Corresponding author. Tel.: +88-01676110465
E-mail address: showrove.hasan@gmail.com

Continuity equation:

$$\frac{\partial Vr}{\partial r}+\frac{Vr}{r}+\frac{\partial Vz}{\partial z}=0$$

Momentum equation:

r- Momentum

$$\frac{\partial Vr}{\partial t}+\frac{\partial (Vr)^2}{\partial r}+\frac{\partial (VzVr)}{\partial z}+\frac{(Vr)^2\_(V\theta)^2}{r}$$
$$=\frac{\partial P1}{\partial r}+\frac{2}{Re}\frac{\partial}{\partial r}\left(\mu eff\frac{\partial Vr}{\partial r}\right)$$
$$+\frac{2}{Re}\frac{\mu eff}{r}\left(\frac{\partial Vr}{\partial r}-\frac{Vr}{r}\right)$$
$$+\frac{1}{Re}\frac{\partial}{\partial z}\{\mu eff\left(\frac{\partial Vz}{\partial r}+\frac{\partial Vr}{\partial z}\right)\}$$

z- Momentum

$$\frac{\partial Vz}{\partial t}+\frac{\partial}{\partial r}(VrVz)+\frac{\partial}{\partial z}(Vz)^2+\frac{VrVz}{r}$$
$$=-\frac{\partial P1}{\partial z}$$
$$+\frac{1}{Re}\frac{1}{r}\frac{\partial}{\partial r}\left\{r\mu eff\left(\frac{\partial Vr}{\partial r}+\frac{\partial Vr}{\partial z}\right)\right\}$$
$$+\frac{2}{Re}\frac{\partial}{\partial z}(\mu eff\frac{\partial Vz}{\partial z})$$

θ- Momentum

$$\frac{\partial V\theta}{\partial t}+\frac{\partial}{\partial r}(VrV\theta)+\frac{\partial}{\partial z}(VzV\theta)+\frac{2Vr}{r}V\theta$$
$$=\frac{1}{Re}\frac{1}{rr}\frac{\partial}{\partial r}\left\{r\mu eff\left(\frac{\partial V\theta}{\partial r}+\frac{V\theta}{r}\right)\right\}$$
$$+\frac{1}{Re}\frac{\partial}{\partial z}(\mu eff\frac{\partial V\theta}{\partial z})$$

Where, $P_1 = p+\frac{2}{3}\kappa$

$\mu eff = 1+\mu_t$

$\mu_t = \frac{C\mu Re\,\kappa^2}{\varepsilon}$

Turbulent kinetic energy equation:

$$\frac{\partial \kappa}{\partial t}+\frac{\partial}{\partial t}(Vr\ \kappa)+\frac{\partial}{\partial z}(Vz\,\kappa)+\frac{Vr\,\kappa}{r}$$
$$=\frac{1}{Re}\frac{1}{r}\frac{\partial}{\partial r}\left(r\frac{\mu_t}{\sigma_\kappa}\frac{\partial \kappa}{\partial r}\right)$$
$$+\frac{1}{Re}\frac{\partial}{\partial z}\left(\frac{\mu_t}{\sigma_\kappa}\frac{\partial \kappa}{\partial z}\right)$$
$$+\frac{1}{Re}\mu\left[2\left\{\left(\frac{\partial V_t}{\partial r}\right)^2+\left(\frac{Vr}{r}\right)^2\right.\right.$$
$$\left.+\left(\frac{\partial Vz}{\partial z}\right)^2\right\}+\left(\frac{\partial V\theta}{\partial r}-\frac{V\theta}{r}\right)^2$$
$$\left.+\left(\frac{\partial Vr}{\partial z}+\frac{\partial Vz}{\partial r}\right)^2+\left(\frac{\partial V\theta}{\partial z}\right)^2\right]$$
$$-\varepsilon$$

Turbulent kinetic energy dissipation rate equation:

$$\frac{\partial \varepsilon}{\partial t}+\frac{\partial}{\partial r}(Vr\,\varepsilon)+\frac{\partial}{\partial z}(Vz\varepsilon)+\frac{Vr\,\varepsilon}{r}$$
$$=\frac{1}{Re}\frac{1}{r}\frac{\partial}{\partial r}\left(r\frac{\mu_t}{\sigma_\varepsilon}\frac{\partial \varepsilon}{\partial r}\right)$$
$$+\frac{1}{Re}\frac{\partial}{\partial z}\left(\frac{\mu_t}{\sigma_\varepsilon}\frac{\partial \varepsilon}{\partial z}\right)$$
$$+\frac{1}{Re}C_{1\varepsilon}\frac{\varepsilon\mu_t}{\kappa}\left[2\left\{\left(\frac{\partial Vr}{\partial r}\right)^2\right.\right.$$
$$\left.+\left(\frac{Vr}{r}\right)^2+\left(\frac{\partial Vz}{\partial z}\right)^2\right\}$$
$$+\left(\frac{\partial V\theta}{\partial r}-\frac{V\theta}{r}\right)^2$$
$$\left.+\left(\frac{\partial Vr}{\partial z}+\frac{\partial Vz}{\partial r}\right)^2+\left(\frac{\partial V\theta}{\partial z}\right)^2\right]$$
$$-C_{2\varepsilon}\frac{\varepsilon^2}{\kappa}$$

2.2. Boundary conditions

The numerical solution domain for an axisymmetric pipe flow problem can be written as $0\leq r\leq R$; $0\leq z\leq L$. Which is a rectangle shown in **Fig.2**.The corresponding boundaries are also indicated in the **Fig.2**.If we rotate the rectangle 360^0 about the axis, we obtain the three dimension pipe geometry.

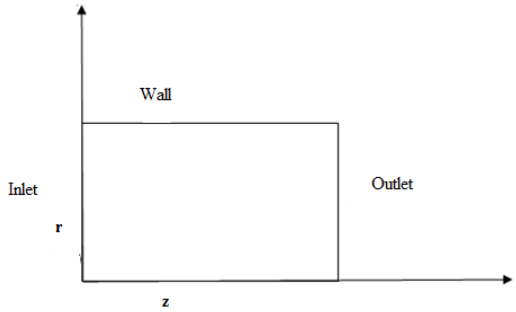

Fig.2 The problem domain and boundaries for axisymmetric pipe flow problem.

Inlet: $V_z = 1$, $V_r = 0$, $V_\theta = 0$, $\kappa = \kappa_{in}$ and $\varepsilon = \varepsilon_{in}$

Outlet: $\frac{d\phi}{dz} = 0$, Where $\phi = V_r, V_z, V_\theta, \kappa$ and ε

Wall: $V_z = V_r = V_\theta = 0$, logarithmic law of wall

Axis:

$$\frac{\partial Vz}{\partial r} = Vr = V_\theta = 0$$

Orifice:

When z = 80 then, from r = 0.25 to r = 0.5

$V_r = 0$ and Vz = 0

When r = 0.25 then, from z = 80 to z = 80.1Vr = 0

When z = 80.1 then, from r = 0.25 to r = 0.5

$V_r = 0$

3. Numerical Experimentation

The numerical code is applied to observe the flow field in a circular pipe. The fully developed length is found as 3.45. The fully developed velocity profile is found at that length in numerical computation. So, the numerical code is valid for fully developed length. The fully developed velocity profile is shown in the following figures for discharge, Q = $0.01 m^3/s$.

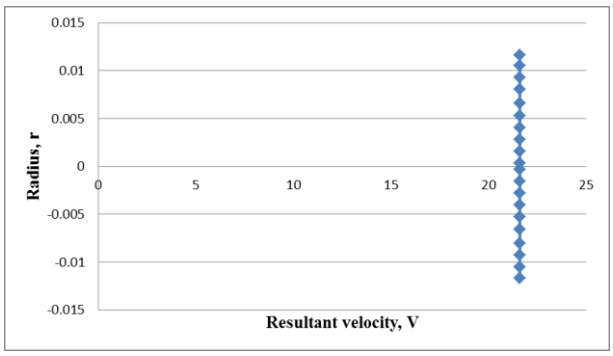

Fig.3 Velocity profile at distance z = 1.2 for Reynolds number, Re = 509296.22.

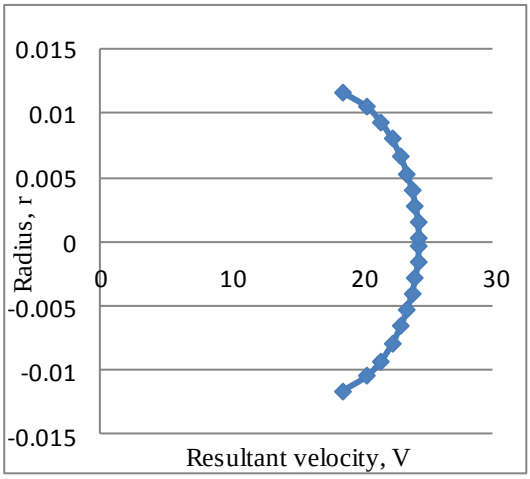

Fig.4 Velocity profile at distance z = 88.6 for Reynolds number, Re = 509296.22.

From the above figures it may be said that not all fluid particles travel at the same velocity within a pipe. The shape of the velocity curve (the velocity profile across any given section of the pipe) depends upon whether the flow is laminar or turbulent. If the flow in a pipe is laminar, the velocity distribution at a cross section will be parabolic in shape with the maximum velocity in the center being about the twice the average velocity in the pipe. In turbulent flow, a fairly flow velocity distribution exists across the section of the pipe, with the result that the entire fluid flows at a given single value. The velocity of fluid in contact with the pipe wall is essentially zero and increases the further away from the wall. By analyzing the figures it may be said that velocity profiles varies slightly in shape for turbulent pipe flow. The following figures represent the flow field in an orifice meter of a given geometry and given operating conditions.

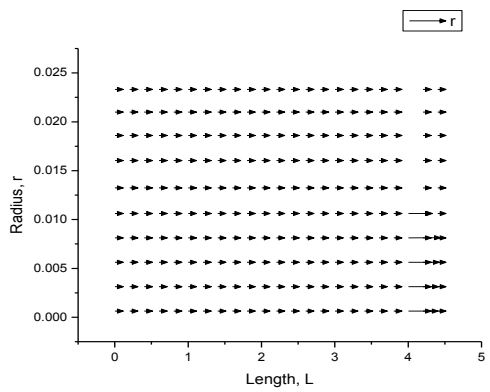

Fig.5 Velocity vector in a circular pipe with an orifice plate for Re=33104.25.

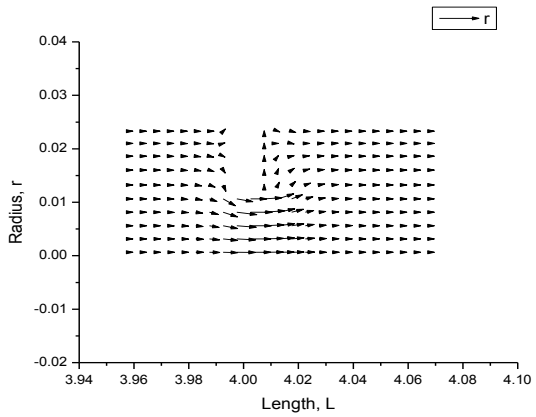

Fig.6 Velocity vector in a circular pipe for Re=33104.25 around the orifice.

Numerical Experimentation was done for the orifice meter in a circular pipe specified dimensions given in **Table 1**.

Table 1 Dimension of orifice meter, pipe and input

Serial No.	Diameter of the Pipe , D(m)	Diameter of the orifice , d(m)	Length of the pipe , L (m)	Flow rate in the pipe , Q (m^3/s)	Reynolds number , Re
1.	0.05	0.025	4.5	0.0013	33104.254
2.				0.0016	40743.698
3.				0.0018	45836.660

The numerical experimentation was done within the following range of Reynolds number $3.3X10^4 < R_e < 4.6X10^4$

Table 2 Numerical results for Q = 0.0013 m^3/sec

Discharge Q (m^3/sec)	Resultant velocity V_{res} (m/s)	Velocity at the end V_{end} (m/s)	Discharge at the end Q_{end} (m^3/s)	Theoretical Discharge Q_{th}(m^3/sec)	Pressure drop $(\Delta P)_{num}$ (Pa)	Coeff. of discharge, $(C_d)_{num}$
0.0013	0.661658	0.661658	0.00129961	0.00210	19492.27	0.61

Table 3 Numerical results for Q = 0.0016 m^3/sec

Discharge Q (m^3/sec)	Resultant velocity V_{res} (m/s)	Velocity at the end V_{end} (m/s)	Discharge at the end Q_{end} (m^3/s)	Theoretical Discharge Q_{th} (m^3/s)	Pressure drop $(\Delta P)_{num}$ (Pa)	Coefficient of discharge, $(C_d)_{num}$
0.0016	0.81469	0.81469	0.0015996	0.002536	24040.691.	0.63

Table 4 Numerical results for Q = 0.0018 m^3/sec

Discharge Q (m^3/s)	Resultant velocity V_{res} (m/s)	Velocity at the end V_{end} (m/s)	Discharge at the end Q_{end} (m^3/s)	Theoretical Discharge Q_{th} (m^3/s)	Pressure drop $(\Delta P)_{num}$ (Pa)	Coefficient of discharge, $(C_d)_{num}$
0.0018	0.91731	0.91731	0.0018	0.002918	45836.660	0.64

4. Experimental setup

A 0.5 m diameter pipe of 4.5 m long was used for the construction of orifice meter. An orifice plate with an orifice diameter 0.25 m was placed inside the 0.5 m diameter pipe. Two pressure tapping points one at 1.5 D before the orifice plate and other at 0.5 D after the orifice plate were constructed to connect with a U-tube differential manometer for the measurement of pressure head difference. Water enters the pipe and finally passes away through the orifice as shown in Fig.6. For every discharge the pressure head difference and discharge readings were recorded.

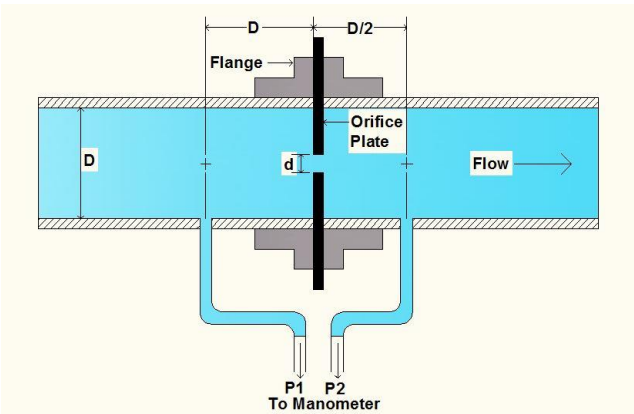

Fig.7 Experimental set up for an orifice meter

5 Experimental Data and Analysis

Table 5 Data for discharge Q = 1.3x10^{-3} m^3/sec.

Serial No.	Vol. of water Liter	Time Sec	Q_{ac} (m^3/sec)	Average Q_{ac} (m^3/sec)	Press. head h cm	Average h cm
1.	20.5	15.76	1.3x 10^{-3}	1.3x 10^{-3}	10.4	10.5
2.		15.70	1.3x 10^{-3}		10.6	
3.		15.77	1.3x 10^{-3}		10.4	
4.		15.77	1.3x 10^{-3}		10.6	
5.		15.75	1.3x 10^{-3}		10.5	

Table 6 Data for discharge Q = 1.6x10^{-3} m^3/sec

Serial no.	Liter	Time (sec)	Q (m^3/sec)	Average Q (m^3/sec)	Pressure head h (cm)	Average h (cm)
1.	20.5	12.81	1.6x 10^{-3}	1.6x 10^{-3}	15.1	15
2.		12.80	1.6x 10^{-3}		15.1	
3.		12.79	1.6x 10^{-3}		14.9	
4.		12.80	1.6x 10^{-3}		14.9	

Table 7 Data for discharge Q = 1.8x10^{-3} m^3/sec

Serial no.	Liter	Time (sec)	Q (m^3/sec)	Average Q (m^3/sec)	Pressure head h (cm)	Average h (cm)
1.	20.5	12.81	1.8x 10^{-3}	1.8x 10^{-3}	18.6	18.5
2.		12.80	1.8x 10^{-3}		18.5	
3.		12.79	1.8x 10^{-3}		18.5	
4.		12.80	1.8x 10^{-3}		18.4	
5.		12.81	1.8x 10^{-3}		18.5	

5.1 Data analysis

Calculation for discharge $Q = 1.3x10^{-3}$ m^3/sec

Pressure drop, $(\Delta P)_{exp} = (P_2-P_1) = h\rho g = 13998.379$ Pa

$Q_{th} = C_c A_o (2gh)^{0.5} = 2.0655x10^{-3}$ m^3/sec

Coefficient of discharge, $C_d = Q/Q_{th}$

$= (1.3x10^{-3})/ (2.0655x10^{-3})$

$= 0.6293$

Similarly, for $Q = 1.6x10^{-3}$ m^3/sec and $1.8x10^{-3}$ m^3/sec C_d values become 0.64 and 0.65

6. Results & Discussion

The different values of C_d for different values of discharges in the range of $1.3x10^{-3}$ to $1.8x10^{-3}$ m^3/sec both for experimental and numerical experimentations have been placed in **Table 8**. It was found that the values of C_d increases with the increase of discharge for both cases. It was also observed that numerically calculated values were always less than experimentally obtained values. **Fig.8** shows the variation of C_d with different discharges. The C_d value was found to increase with the increase of discharge in both cases. Again, experimental values were found higher than the numerical ones.

Table 8 Comparison of experimental and numerical results

Q (m^3/ sec)	Pressure drop $(\Delta P)_{exp}$ (Pa)	Pressure drop $(\Delta P)_{num}$ (Pa)	$(C_d)_{exp}$	$(C_d)_{num}$	$(C_d)_{num}$ is less than $(C_d)_{exp}$ by
0.0013	13998.4	19492.3	0.629	0.617	1.95%
0.0016	19997.685	24040.69	0.64	0.63	1.56%
0.0018	24663.811	31823.56	0.65	0.64	1.54%

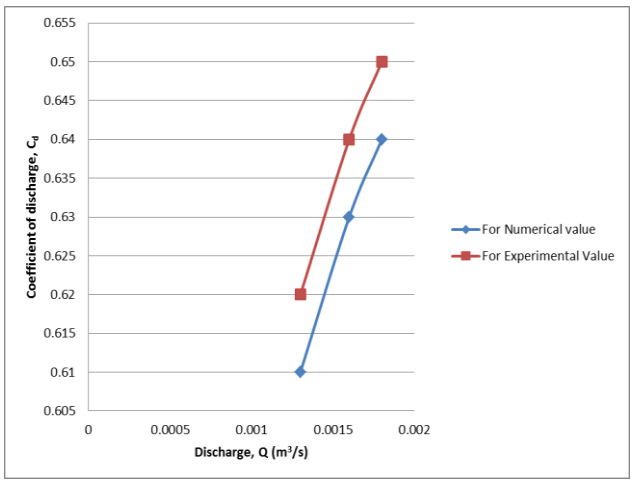

Fig.8 Relation between discharge and coefficient of discharge for numerical and experimental values

7. Conclusion

A numerical code for the computation of coefficient of discharge and pressure drop in an orifice meter through a circular pipe is written and executed by using MAC algorithm in the present work. An experimental set up is fabricated for orifice meter to get experimental values. The numerical results are compared with the experimental results. The following features have been observed

- The coefficient of discharge is found to increase with the increase of discharge or Reynolds number in both experimental and numerical studies
- The values of coefficient of discharge, C_d from experimental study are always found higher than that of in the numerical study and the maximum deviation is found 1.95%

NOMENCLATURE

V_z: Velocity in z direction, m/s
V_r: Velocity in r direction, m/s
P: Pressure drop, N/m^2
ΔP: Change in pressure, N/m^2
∂t: Time step, sec
μ: Viscosity, N.s/ m^2
Q: Actual volume flow rate, m^3/s
Q_{th}: Theoretical volume flow rate, m^3/s
A: Area of pipe, m^2
A_o: Area of orifice, m^2
ρ: Density of fluid, Kg/ m^2
D: Diameter of pipe, m
d : Diameter of orifice, m
τ_w :Wall shear stress
Re: Reynolds number
κ: Turbulent kinetic energy, J
ε: Turbulent kinetic energy dissipation rate, W/m^2
$C\mu, C_{1\varepsilon}, C_{2\varepsilon}$: Empirical constants of κ-ε equations
C_c : Coefficient of contraction
C_d : Coefficient of discharge
Subscript
r: In radial direction
z: In axial direction
Superscript
i: z directional grid
j: r directional grid
Δx: distance between two nodes in z direction
Δy: distance between two nodes in r direction

REFERENCES

[1] Dr. P.N Modi, Dr.S.M Seth, Hydraulics and Fluid Mechanics, Standard Book house, 2006

[2] H K Versteeg, W Malalasekera, An Introduction To Computational Fluid Dynamics.

[3] K Muralidhar, T Sundararajan, Computational Fluid Flow and Heat Transfer, Narosa, 2nd Edition

[4] John D. Anderson. Jr, Computational Fluid Dynamics, McGraw-Hill International Edition.

[5] Pervin, M.S.A, Halder, M.R. Numerical Modeling on Solid Cone Nozzle without a Vane Swirled, Paper 06.